ChinaXiv合作期刊

Nuclear Science and Techniques **24** (2013) 020102

An experimental study of dual-energy CT imaging using synchrotron radiation

HAO Jia[1,2] ZHANG Li[1,2] XING Yuxiang[1,2] KANG Kejun[1,2]

[1]*Department of Engineering Physics, Tsinghua University, Beijing 100084, China*

[2]*Key Laboratory of Particle & Radiation Imaging (Tsinghua University), Ministry of Education, Beijing 100084, China*

Abstract The measurement of electron density is important for medical diagnosis and charged particle radiotherapy treatment planning. Traditionally, electron density is obtained by CT imaging using the relationship between CT-number and electron densities established beforehand. However, the measurement is not accurate due to the beam hardening effect. In this paper, we propose a simple and practical electron density acquisition method based on dual-energy CT technique. For each sample, the CT imaging is conducted using two selected X-ray energy from synchrotron radiation. A post-processing dual-energy reconstruction method is used. Linear attenuation coefficients of the scanned samples are obtained by FBP reconstruction. The effective atomic number and electron density are got by solving the dual-energy simultaneous equations. Different phantoms and breast tissues were scanned in this experimental study under 10 keV and 30 keV monochromatic X-rays. The distribution of effective atomic numbers and electron densities of the scanned phantoms were obtained by Dual-energy CT image reconstruction, which agrees well with the theoretical values. Compared with conventional methods, the measurement accuracy is greatly improved, and the measurement error is reduced to about 1%. This experimental study demonstrates that DECT imaging based on synchrotron radiation source is applicable to medical diagnosis for quantitative measurement with high accuracy.

Key words Dual-energy CT, Synchrotron radiation, Electron density, X-ray imaging

chinaXiv:202306.00200v1

1 Introduction

Nowadays, computed tomography (CT) has become a mainstay for medical imaging and nondestructive testing in modern radiology. The internal structure of an object can be exactly reconstructed from CT scanning projections. The electron density is important in photon and charged particle radiotherapy[1]. Traditionally, this information is obtained by CT imaging using the relationship between CT-number (in Housfield units) and electron densities established beforehand[2]. However, a conventional CT system, which uses X-ray tube, inherently has a broad energy spectrum. The resulting CT number has some uncertainties due to beam hardening effect. Thus, the accuracy of electron density measurement is degraded.

The dual-energy CT (DECT) was proposed by Alvarez[3] in 1976. Using X-ray under two different tube energies, the information of electron density and effective atomic number of inspected objects can be derived. This technique has been widely used in medical and industrial applications, especially in safety check and material discrimination. All the proposed dual-energy reconstruction methods can be broadly classified into three groups: pre-processing, post-processing and iterative reconstruction methods[4]. In polychromatic X-ray DECT systems, the pre-processing methods are widely used to avoid beam-hardening effects. The post-processing reconstruction methods have their advantages in computational simplicity. The iterative reconstruction methods based on statistical model and non-statistical model yield a high signal noise ratio[5]. However, the great computation cost decreases their practicability. In China, the different groups focus on the DECT techniques. Zhang *et al.*[6] proposed a practical DECT

* Corresponding author. *E-mail address*: zli@mail.tsinghua.edu.cn

Received date: 2012-08-05

ChinaXiv合作期刊

chinaXiv:202306.00200v1

reconstruction method based on spectrum estimation, thus obtaining the distribution of effective atomic numbers and electron densities from polychromatic X-ray projections under two tube voltages. Most of the research groups focused on the clinical application and evaluation of DECT[7].

Because X-rays from synchrotron radiation source are highly monochromized, the effects of beam-hardening in CT imaging can be ignored. Hence, synchrotron radiation CT (SRCT) can better detect low-contrast lesions and obtain better image quantification than conventional CT. In 1997, Dilmanian *et al.*[8] conducted single and multi-energy CT at the National Synchrotron Light Source, Brookhaven, USA. They compared the image noise between SRCT and conventional CT. In 2010, Chen *et al.*[9] measured the linear attenuation coefficients of surgical breast tissues by SRCT in the energy range of 15.0 to 26.5 keV at the SYRMEP beamline of the ELETTRA SR facility in Trieste, Italy. Torikoshi *et al.*[10–12] and Tsunoo *et al.*[13] presented a method for DECT using monochromatic X-rays from Spring-8 in Japan, thus claiming to measure the electron density with accuracy of around 1%[14]. In China, the SSRF (Shanghai Synchrotron Radiation Facility) is a third-generation of synchrotron radiation light source. With the electron beam energy of 3.5 GeV, it is the fourth energy high in the world and offers X-ray with high intensity, high brilliant, high polarization and high stability[15], and it serves as an scientific platform for science research and technology development[16,17].

In this paper, a simple but practical measurement method is proposed. A DECT imaging experiment is designed using synchrotron radiation to explore its potential medical applications, and carried out at beamline BL13W1 of SSRF.

2 DECT reconstruction method

Synchrotron radiation source provides highly monochromatic X-rays with continuously adjustable energies. Thus, the pre- and post-processing dual-energy reconstruction methods give similar results. For the purpose of simplicity in implementation, a post-processing dual-energy reconstruction method was used in our experiment. First, linear attenuation coefficients of the scanned samples are obtained using CT reconstruction using the two selected X-ray energies. Then the effective atomic number and electron density are solved from dual-energy simultaneous equations.

In the photon energy range normally used in medical imaging, the linear attenuation coefficient μ can be approximately expressed as a linear combination of photoelectric interaction term and Compton scattering term as follows[18].

$$\mu \approx 0.5K_1N_A f_{\mathrm{ph}}(E)Z^n\rho_{\mathrm{e}}+0.5K_2N_A f_{\mathrm{KN}}(E)\rho_{\mathrm{e}} \quad (1)$$

where $f_{\mathrm{ph}}(E)$ and $f_{\mathrm{KN}}(E)$ as functions of the X-ray energy are the energy-dependent photoelectric interaction and Compton scattering, respectively. The n (≈4) is a constant. The variable Z is the atomic number, and N_{A} is the Avogadro's number. K_1 and K_2 are constants related to the photoelectric interaction and the Compton scattering. ρ_{e} is electron density (g/cm^3) and can be expressed as

$$\rho_{\mathrm{e}} = 2\rho Z/A \quad (2)$$

where ρ is the mass density (g/cm^3) and A is the atomic weight. For compounds, the effective atomic number (Z_{eff}) is used instead of Z, and defined as

$$Z_{\mathrm{eff}} = \left[\sum_i c_i Z_i^{n+1} / \sum_i c_i Z_i \right]^{1/n}. \quad (3)$$

where c_i is the number of atoms for the i^{th} element in the molecule of the compound and Z_i is the atomic number of the i^{th} element. Eq.(1) can be simplified to

$$\mu(E) = \alpha_1 f_{\mathrm{ph}}(E)Z^n\rho_{\mathrm{e}} + \alpha_2 f_{\mathrm{KN}}(E)\rho_{\mathrm{e}} \quad (4)$$

a_1 and a_2 as constants are defined as follows.

$$\alpha_1 = 0.5K_1N_A, \ \alpha_2 = 0.5K_2N_A \quad (5)$$

Scanning with dual X-ray energies E_L and E_H, the linear attenuation coefficients $\mu(E_L)$ and $\mu(E_H)$ can be obtained by the filtered back-projection (FBP) reconstruction method. We can derive dual-energy simultaneous equations from Eq.(4), as follows

$$\begin{aligned} \mu(E_L) &= \alpha_1 f_{\mathrm{ph}}(E_L)Z^n\rho_{\mathrm{e}} + \alpha_2 f_{\mathrm{KN}}(E_L)\rho_{\mathrm{e}} \\ \mu(E_H) &= \alpha_1 f_{\mathrm{ph}}(E_H)Z^n\rho_{\mathrm{e}} + \alpha_2 f_{\mathrm{KN}}(E_L)\rho_{\mathrm{e}} \end{aligned} \quad (6)$$

Solving the simultaneous Eq.(6) gives Eq.(7).

$$Z_{\mathrm{eff}}{}^n = [\alpha_2 f_{\mathrm{KN}}(E_L)\,\mu(E_H) - \alpha_2 f_{\mathrm{KN}}(E_H)\,\mu(E_L)] / [\alpha_1 f_{\mathrm{ph}}(E_H)\,\mu(E_L) - \alpha_1 f_{\mathrm{ph}}(E_L)\,\mu(E_H)] \quad (7)$$

ChinaXiv合作期刊

$$\rho_e=[\mu(E_L)-\mu(E_H)]/\{\alpha_1[f_{ph}(E_L)-f_{ph}(E_H)]Z_{eff}^n+\alpha_2[f_{KN}(E_L)-f_{KN}(E_H)]\} \quad (8)$$

This method is available for low Z elements, but not high Z elements because they have absorption edges in the used energy region. Simulation study has been conducted by a numerical phantom consisting of different materials, indicating that the electron density can be obtained by high accuracy using the proposed dual-energy reconstruction method[19].

3 DECT experiment at SSRF

3.1 Beamline and CT system

For X-ray imaging and biomedical application, the monochromatic X-ray CT imaging system in beamline BL13W1 of SSRF is shown in Fig.1. The two-dimensional (2D) CCD detector used in this experiment has 4000×2500 pixels, and its spatial resolution reached 13 μm. Samples were placed on a rotation table approximately 30 m downstream source. Synchrotron radiation with a continuous energy spectrum was monochromatized with a double-crystal monochromator. BL13W1 is equipped with mono-chromator Si(111) and Si(311). In this experiment, Si(111) was used. The maximal photon flux density appears at the X-ray energy of 20 keV. A collimator in the system is used to prevent the scattering photon and improve the accuracy of reconstructed results.

In DECT, it is intuitive to choose low/high energy as far from each other as possible. Because too-low X-ray energy would increase image noise, the 10 keV and 30 keV were chosen as the low/high energy. In order to ensure the same object position in scanning, each sample should take DECT twice under 10 keV and 30 keV monochromatic X-rays alternately, and scan another sample. The low-energy X-ray absorption images were taken first within the π angular range under 10 keV. Then the sample was rotated backward to the beginning along the vertical axis. The X-ray energy was changed to 30 keV for next scanning. For each CT scan, the total number of views was 540 covering the π angle range. The data acquisition time and exposure, which depend on the photon flux density, takes about 2–4 min per CT scanning. It is necessary to slowly rotate the scanned object to prevent motion artifacts. The refraction effect can enhance the material boundaries and the image contrast, but also could cause inaccuracy in the electron density images. We shorten the object to detector distance at less than 10 cm to eliminate the boundary enhancement in the reconstruction images.

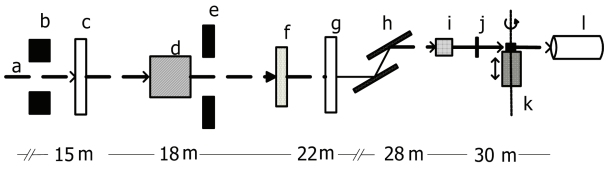

Fig.1 A schematic drawing of the experimental system for CT imaging in the beamline BL13W1 at SSRF. (a) White beam, (b) diaphragm, (c) filter 1, (d) γ collimator, (e) white beam slit, (f) berrilium window, (g) filter 2, (h) DCM (Double-crystal monochromator), (i) photon shutter, (j) γ collimator, (k) rotation table, (l) 2-D X-ray detector.

Table 1 Parameters of Beamline BL13W1 at SSRF

Items	parameters
Beam model	Unfocused monochromatic beam
Imaging method	PCI, Micro CT
Energy range(KeV)	8–72.5
Energy resolution(ΔE/E)	$\leq 5\times10^{-3}$
Maximal beam size(mm)	45 (H)×5(V)
Photon flux density using Si(111) (phs/s/mm^2 @20keV@200mA)	1×10^9
Max time resolution(ms/frame)	1.0

3.2 Samples

To evaluate the reconstructions and provide necessary correction, Water, alcohol, and polyethylene cylinder as phantoms are used to quantitatively evaluate the discrepancies between the measured and theoretical values. All the samples were scanned in plastic tubes of 18-mm diameter.

Water phantoms are used for calibration of electron density and correcting the systematic error. By water calibration, the reconstructed electron density value is multiplied by 1.03, which is the ratio of the measured to theoretical attenuation coefficients. The deviation mainly comes from the influence of noise and the nonlinearity in the detector response

chinaXiv:202306.00200v1

ChinaXiv合作期刊

function. Also, the theoretical process to derive from dual-energy linear attenuation coefficients may introduce error in the electron density measurement. In addition, the breast tissues in plastic tubes were used to investigate the feasibility of synchrotron radiation DECT in clinical application.

3.3 Data processing

Images without a sample are taken before and after each CT scanning to be I_0 in reconstruction. X-ray energies of 10 keV and 30 keV are used in the DECT experiments. For each sample, two linear attenuation coefficient images with dual-energy X-ray are reconstructed by parallel-beam FBP method using the Shepp-Logan filter function after the dark-field and flat-field corrections. Electron density and effective atomic number of each pixel are calculated by the proposed reconstruction method. Solving Eq.(8), the coherent scattering term is calculated from standard element oxygen. The oxygen cross-sections were quoted from database[20].

In practical scanning, the data acquisition always suffers from noises and detector nonlinearity. Therefore, after retrieval of the attenuation coefficient maps from the raw projection data, total variation minimization method is used for noise reduction[21]. The computation from Eqs.(7) and (8) for the air part in the scanning FOV could result in a big unexpected error because the divisor is close to zero. Hence, we directly set the electron density in air region to a small value of 1×10^{-4}.

4 Results and Discussion

In order to quantitatively evaluate the accuracy, we first used different cylinder phantoms including water, polyethylene and alcohol. Table 2 contrasts the measured and theoretical results. The theoretical values of effective atomic numbers and electron densities come from NIST standard reference database [20]. For water and polyethylene phantom, the average value of measured electron density is fairly consistent with the theoretical ones (about 1% error). The electron density measured by synchrotron radiation DECT is sufficiently good, thus improving the precision of the treatment planning for radiotherapy. An effective atomic number image was obtained as a byproduct from DECT.

Table 2 Experimental results of effective atomic numbers and electron densities of scanned phantoms

	Effective atomic number			Electron density (g/cm^3)		
	Measured	Theoretical	Relative accuracy / %	Measured	Theoretical	Relative accuracy / %
Water	7.52	7.51	0.13	1.11	1.11	/
Polyethylene	5.57	5.52	0.91	1.07	1.06	0.93
Alcohol	6.53	6.47	0.93	0.90	0.89	1.12

Figure 2 shows the electron density (a) and atomic number distribution images (b) of a breast tissue sample with pathological changes. The dark background is the air part in the tube. We can find a big difference between the two images. The image of electron density shows a striking contrast between normal and abnormal tissue, and are rather similar in the effective atomic number image. The information may give different criteria for the discrimination of abnormal tissues from normal tissues. Since the quantitative information about breast tissues is not currently available, we just calculated their average in different ROI. After statistics, the average electron density in the ROI1 area is 1.11 g/cm^3; and 1.02 g/cm^3 in the ROI2 area.

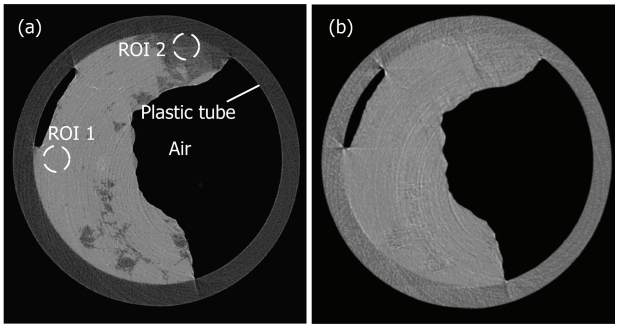

Fig.2 Electron density ρ_e reconstruction results of breast tissue sample at the grayscale range of [0.8, 1.5] (g/cm^3) (a). Effective atomic number Z reconstruction results of a breast tissue sample at the grayscale range of [1,15] (b).

chinaXiv:202306.00200v1

ChinaXiv合作期刊

5 Conclusions

The precise measurement of electron densities is essential in treatment planning for hadron therapy. The most popular way is to convert the CT numbers to electron densities by establishing their relationship in spite of that it is not accurate enough. The SSRF has great potential for quantitative medical diagnosis and provide an excellent platform for X-ray imaging research. We conducted a DECT experiment to evaluate the accuracy and clinical application of electron density measurement with synchrotron radiation. Different phantoms and samples are investigated. The electron density reconstruction results of phantoms agree to the theoretical ones with high precision after correction, thus satisfying the heavy-ion and proton radiotherapy. Currently, the beamlines in SSRF is only available for research, and the SSRF should be designed for medical applications in the future. The DECT with synchrotron radiation has the potential to be an important tool in clinical performances. We will further study on this area, such as noise reduction methods, dose evaluation and clinical application research.

Acknowledgements

This work is supported by National Key Technology R&D Program of the Ministry of Science and Technology (No. 2012BAI07B05). The authors thank Xiao Tiqiao and Xie Honglan from Shanghai Institute of Applied Physics, Chinese Academy of Sciences, for their proposal and help in the experiments. We also thank all the staff at beamline BL13W of SSRF for their kind support.

References

1 Dobbs H J, Parker R P, Hodson N J, *et al.* Radiother Oncol, 1983, **1:** 133–141.

2 Matsufuji N, Tomura H, Futami Y, *et al.* Phys Med Biol, 1998, **43:** 3261–3275.

3 Alvarez R, Macovski A. Phys Med Biol, 1976, **21:** 733–744.

4 Engler P, Friedman D. Mater Eval, 1990, **48:** 623–629.

5 Fessler J A, Elbakri I, Sukovic P, *et al.* Proceedings of SPIE medical imaging, 2002, **4684:**38–49.

6 Zhang G W, Cheng J P, Zhang L, *et al.* J X-Ray Sci Technol, 2008, **16:** 67–88.

7 Zhang L J, Chai X, Wu S Y, *et al.* Eur Radiol, 2009, **19:** 2844–2854.

8 Dilmanian F A., Wu X Y, Parsons E C, *et al.* Phys Med Biol, 1997, **42:** 371–387.

9 Chen R C, Longo R, Rigon L, *et al.* Phys Med Biol, 2010, **55:** 4993–5005.

10 Torikoshi M, Tsunoo T, Ohno Y, *et al.* Nucl Instrum Meth A, 2005, **54:** 99–105.

11 Torikoshi M, Tsunoo T, Endo M, *et al.* J Biomed Opt, 2001, **6:** 371–377.

12 Torikoshi M, Tsunoo T, Sasaki M, *et al.* Phys Med Biol, 2003, **48:** 673–685.

13 Tsunoo T, Torikoshi M, Sasaki M, *et al.* IEEE Tran Nuc Sci, 2003, **50:** 1678–1682.

14 Tsunoo T, Torikoshi M, Ohno Y, *et al.* Med Phys, 2008, **35:** 4924–4932.

15 Jiang M H, Yang X, Xu H, *et al.* Chin Sci Bull, 2009, **54:** 4171–4181.

16 Deng B, Yu X, Li A, *et al.* Nucl Sci Tech, 2007, **18:** 257–260.

17 Fu S, Jiang G. Nucl Sci Tech, 2009, **20:** 325–330.

18 Jackson D F and Hawkes D J. Phys Rep, 1981, **70:** 169–233.

19 Hao J, Zhang L, Xing Y, *et al.* J Tsinghua Univ (Sci & Tech), 2011, **51:** 457–461.

20 Hubbell JH, Seltzer S M. NIST Standard Reference Database 126, http://www.nist.gov/pml/data/xraycoef/index.cfm (September 29, 2011).

21 Vese L A, Osher S J. J Math Imaging Vis, 2004, **20:** 7–18.

chinaXiv:202306.00200v1